LASER INTERFEROMETER GRAVITATIONAL WAVE OBSERVATORY
- LIGO -
CALIFORNIA INSTITUTE OF TECHNOLOGY
MASSACHUSETTS INSTITUTE OF TECHNOLOGY

Technical Note	**LIGO-T020059-v3-**	2010/12/29

Are Reaction Chains Needed for aLIGO HAM Optics?

J. Kissel, N. Roberston, M. Barton, P. Willems

California Institute of Technology
LIGO Project, MS 18-34
Pasadena, CA 91125
Phone (626) 395-2129
Fax (626) 304-9834
E-mail: info@ligo.caltech.edu

Massachusetts Institute of Technology
LIGO Project, Room NW17-161
Cambridge, MA 02139
Phone (617) 253-4824
Fax (617) 253-7014
E-mail: info@ligo.mit.edu

LIGO Hanford Observatory
Route 10, Mile Marker 2
Richland, WA 99352
Phone (509) 372-8106
Fax (509) 372-8137
E-mail: info@ligo.caltech.edu

LIGO Livingston Observatory
19100 LIGO Lane
Livingston, LA 70754
Phone (225) 686-3100
Fax (225) 686-7189
E-mail: info@ligo.caltech.edu

Abstract

Willems (2002) had concluded the noise induced on the second and third stages of the HAM triple suspensions by controlling them with iLIGO-style OSEMs mounted directly to the cage is ~ 4 orders of magnitude below the required displacement noise, and therefore reaction chains are not needed for the HAM triple suspensions. In this document we update the calculations made originally by Willems to be sure these conclusions still hold. These updates include final design parameters for the HAM triple suspensions, final design requirements for their displacement in the aLIGO recycling cavities, and updated performance results and requirements for the HAM isolation platform. We conclude that this noise will be at worst is a factor of ~ 5 away from the final length requirements (around HEPI support structure resonances) but typically around a factor of 60 – and that no immediate action need be taken.

1 Introduction

Willems (2002) attempted to answer the question "Are reaction chains needed for aLIGO HAM Optics?" when the conceptual designs for the aLIGO HAM Small Triple Suspension (HSTS), and HAM Large Triple Suspension (HSTS) (then called "MC Triple" and "RM Triple," respectively) were being developed. The question was posed because the conceptual design was to be adapted from the GEO Test Mass Triple Suspension design, which uses a reaction chain as a quiet platform from which to apply actuation forces on the main, test mass chain. Needless to say, it would greatly simplify the design if no reaction chains were needed. Based on the (2002) knowledge that

(a) The requirements for isolation of the recycling cavities are not as stringent as the GEO test masses,

(b) The (then two-stage) isolation platform on which the suspensions sit will be "quite low," and

(c) The design properties of the suspensions were still in the conceptual stage,

Willems concluded that the noise introduced by controlling (with maximum possible force) the middle and bottom stages with OSEMs attached directly to the cage was ~ 4 orders of magnitude away from the required motion of the mode cleaner and recycling cavities.

In this document, we update the calculations made by Willems, using the final design parameters and complete models of the HSTS and HLTS, their final displacement requirements, and updated input motion from the (now single-stage) HAM ISI (both its measurements and requirements). In Section 2, we review Willems equations that calculate the worst-case control noise and demonstrate where the model has been updated, in Section 3 we compare HAM ISI input platform motion, models of the triple suspensions, and the parameters originally used with that of the final designs in aLIGO, in Section 4 we compare the results of the updated calculations, and Section 5 we conclude that everything will be better in Advanced LIGO.

2 Noise Model

We first review Willems' model for the force noise coupling of various terms onto the bottom mass. We restate the model here for convenience, with a few terms more explicitly labeled for clarity. The subscripts or superscripts "T," "M," and "B" are indicative of terms involving the top, middle, and bottom mass, respectively. Where necessary, after each Willems' model equation, we describe improvements to the model. Both models are identical between the HSTS and HLTS; only input parameters and transfer functions unique to either are varied. Note that they do not take into account offloading control to previous stages of isolation, in such a way that we could reduce the actual amount of control needed on the middle or bottom mass. Hence, each are a "worst-case" scenario, in which all stages of the suspension must be driven at the maximum capacity of the OSEM coil driver.

In both models, the longitudinal displacement noise requirements of the bottom mass of the suspension, $x_B^{req}(f)$, are related to force noise requirements, $F_B^{req}(f)$, by assuming a simple equation of motion for the bottom mass,

$$F_B^{req}(f) \quad = \quad m_B\ \omega^2\ x_B^{req}(f) \tag{1}$$

where m_B is the mass of the bottom mass, and ω is the angular frequency (band) of concern.

In T020059-v1, the noise coupling from the third stage's OSEMs (mounted to the cage) to the bottom mass, $F_B^{O\rightarrow B}(f)$, is modeled to be **at worst**

$$F_B^{O\rightarrow B}(f) \quad = \quad F_{max}^{O_B} \times \frac{(dF/dx)}{F} \times x_p(f) \tag{2}$$

with $F_{max}^{O_B} = N_{O_B} I_{O_B}^{req} A_{O_B}$, the maximum possible force exerted by the bottom OSEMs in $[N]$ (N_{O_B} is the number of OSEMs acting on the optic, $I_{O_B}^{req}$ is the dynamic range requirements of the coil drivers in $[A]$, and A_{O_B} is the actuation strength of the coils on the magnets in $[N/A]$ all for the bottom OSEMs), $(dF/dx)/F$ is the gradient of the applied force with displacement in $[1/m]$, and $x_p(f)$ is motion of the platform to which the suspension is mounted (assumed to be the same motion as the cage, and therefore the OSEMs) in $[m/\sqrt{Hz}]$. As with the requirements, this force is converted to displacement assuming a simple equation of motion,

$$x_B^{O\rightarrow B}(f) \quad = \quad \frac{F_B^{O\rightarrow B}(f)}{m_B\ \omega^2} \tag{3}$$

We update this model by computing the displacement noise directly,

$$x_B^{O\rightarrow B}(f) \quad = \quad F_{max}^{O_B} \times \frac{(dF/dx)}{F} \times x_p(f) \times T_{F\rightarrow x}^{B\rightarrow B}(f) \tag{4}$$

where $T_{F\rightarrow x}^{B\rightarrow B}(f)$ is the longitudinal, force-to-displacement transfer function in $[m/N]$, where force is applied directly bottom mass.

The noise coupling from the second stage's OSEMs (also mounted to the cage) to the bottom mass, through the second-to-third stage suspension, $F_B^{O\rightarrow M\rightarrow B}(f)$, is modeled in T020059-v1 (again **at-worst**) to be

$$F_B^{O\rightarrow M\rightarrow B}(f) \quad = \quad F_{max}^{O_M} \times \frac{(dF/dx)}{F} \times x_p(f) \times \left(\frac{f_0}{f}\right)^2 \tag{5}$$

where $F_{max}^{O_M} = N_{O_M} I_{O_M}^{req} A_{O_M}$ is the maximum possible force exerted by the middle OSEMs in $[N]$, and f_0 is the resonant frequency of the second-to-third stage suspension in $[Hz]$. As usual, the force is then converted to displacement,

$$x_B^{O \to M \to B}(f) \quad = \quad \frac{F_B^{O \to M \to B}(f)}{m_B \ \omega^2} \tag{6}$$

Similar to the control from the bottom stage, the model for noise coupling from control of the second stage is updated by computing the displacement noise directly,

$$x_B^{O \to M \to B}(f) \quad = \quad F_{max}^{O_M} \times \frac{(dF/dx)}{F} \times x_p(f) \times T_{F \to x}^{M \to B}(f) \tag{7}$$

with $T_{F \to x}^{M \to B}(f)$ as the longitudinal, force-to-displacement transfer function in $[m/N]$, where force is applied to the middle mass and generating a displacement of the bottom mass.

Finally, for comparison, we include the displacement noise, $x_B^{p \to B}(f)$, of the bottom mass generated by transmission of platform motion, $x_p(f)$, through the triple suspension,

$$x_B^{p \to B}(f) \quad = \quad x_p(f) \times T_{x \to x}^{p \to B}(f) \tag{8}$$

where $T_{x \to x}^{p \to B}(f)$ is the longitudinal, displacement-to-displacement transfer function in $[m/m]$, between the top of the cage (taken to be the same as the platform motion) and the bottom mass. This comparison was not made in T020059-v1, since no such model existed at the time.

3 Parameter Comparison

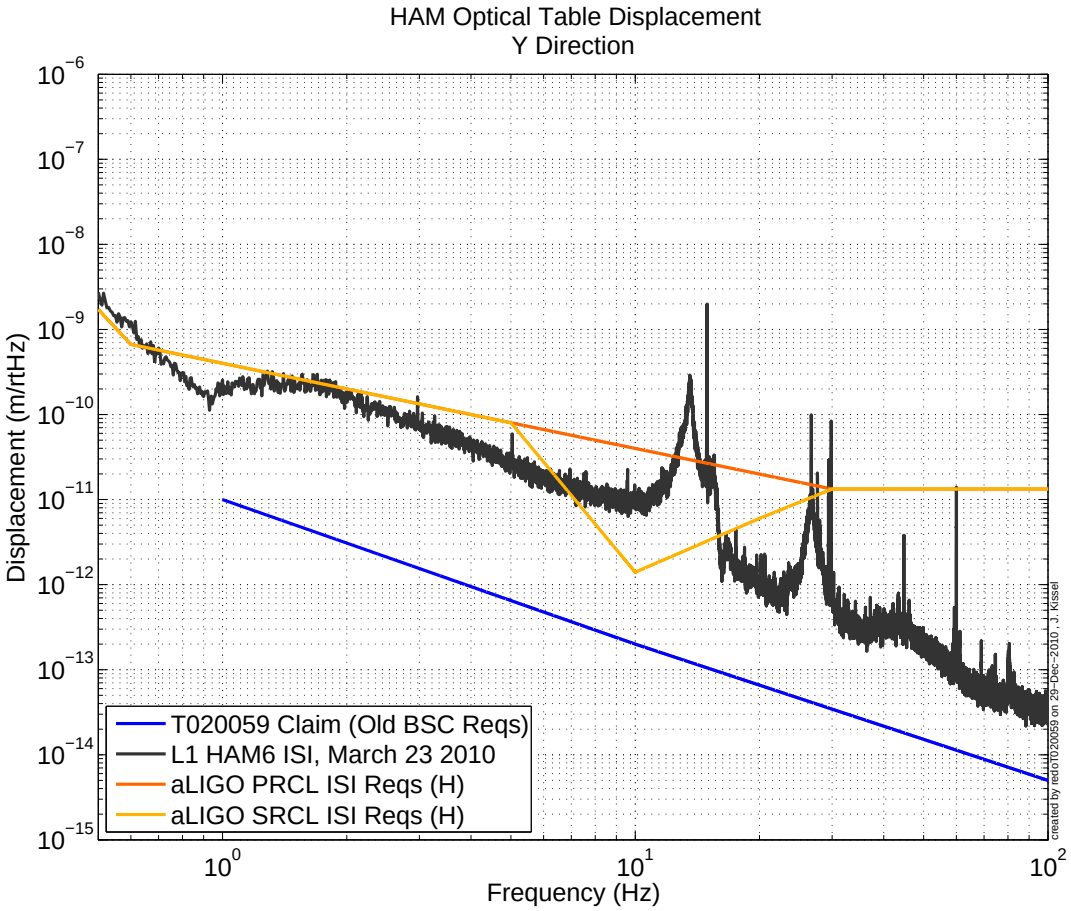

Figure 1: Comparison between requirements and measurements of the HAM isolation platform motion, $x_p(f)$. In blue, that which is defined by T020059-v1 (taken to be the same as the BSC platform, originally defined in E990303); in drak gray, the eLIGO HAM6 ISI performance (in the Y direction); in orange and gold, the requirements defined for the PRCL and SRCL HAM ISI in Advanced LIGO from T1000216, respectively.

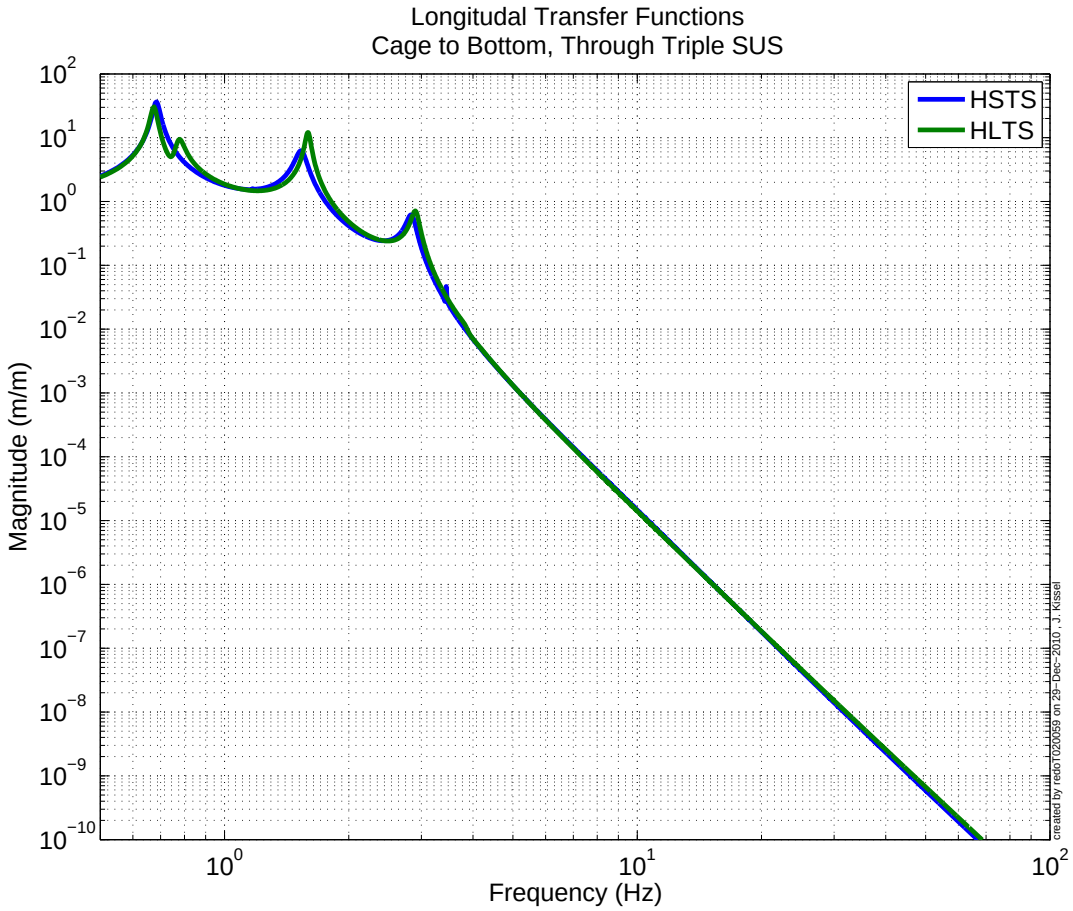

Figure 2: Transmission of HAM ISI input displacement noise through the HSTS and HLTS their respective the bottom masses, $T_{x\rightarrow x}^{p\rightarrow B}$. Models are computed using T080311 and T080310.

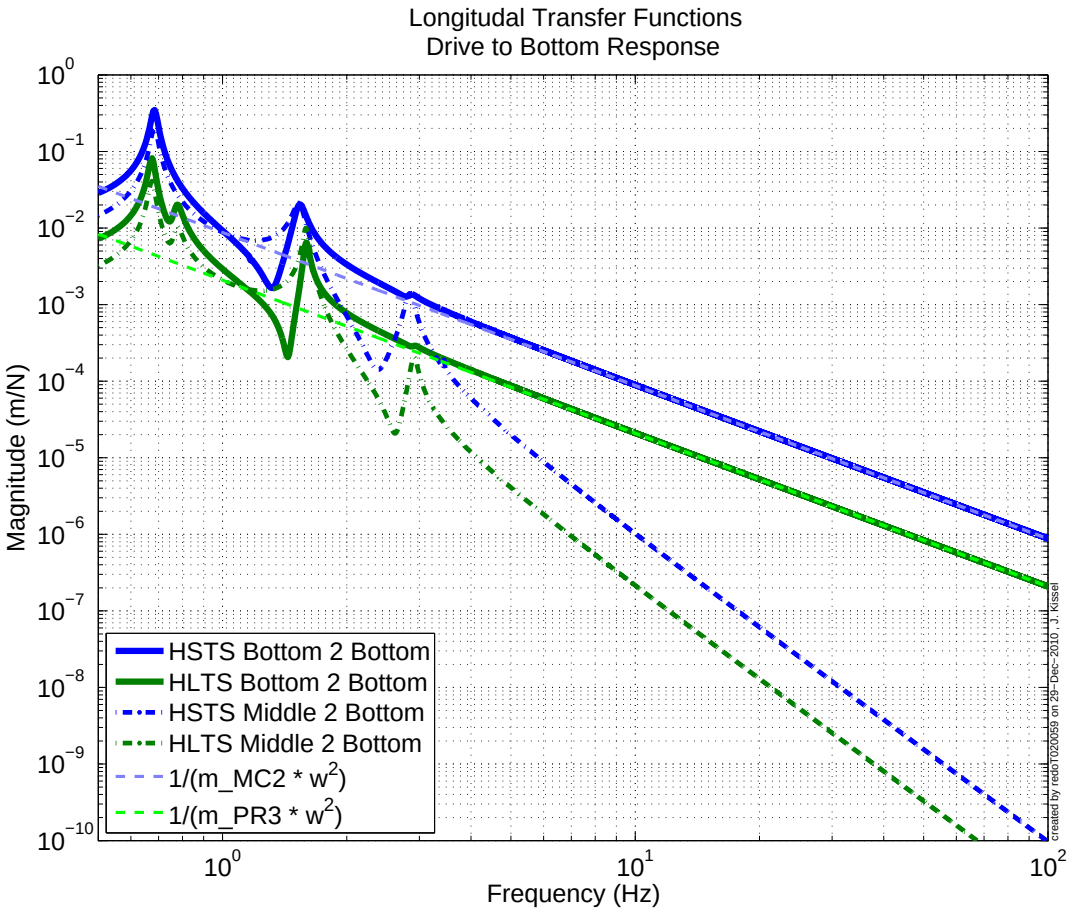

Figure 3: Force-to-displacement transfer functions between force on the bottom mass – either directly on the bottom mass, $T^{B\to B}_{F\to x}$, [solid lines] or on the penultimate mass transmitted through the last suspension stage, $T^{M\to B}_{F\to x}$, [dash-dotted lines] – and the displacement of the bottom mass for both the HSTS and HLTS. Models are computed using T080311 and T080310. As a sanity check, the displacement of a free mass from an applied unit force having the same mass as the mode-cleaner mirrors (for the HSTS) and the large recycling cavity mirrors (for the HLTS) is shown [dashed lines].

Table 1: HSTS Parameter Table.

Parameter	Units	HSTS T020059-v1	HSTS T020059-v2	v2 Reference
$x_B^{req}(f)$	$m\sqrt{Hz}$	3×10^{-17} @ 10 Hz, 3×10^{-19} @ 100 Hz	3×10^{-17} @ 10 Hz, Falling as $f^{-5/2}$	T010007
N_O	–	–	T : 2 M : 4 B : 4	T0900435, Tbl. 1
OSEM Type	–	$T : IOSEM$ $M : IOSEM$ $B : IOSEM$	$T : BOSEM$ $M : AOSEM$ $B : AOSEM$	M0900034, Tbl. 1
Magnet Type, Size	$mm \times mm$	$T : NdFeB, 1.905 \times 3.175$ $M : NdFeB, 1.905 \times 3.175$ $B : NdFeB, 1.905 \times 3.175$	$T : NdFeB, 10 \times 5$ $M : SmCo, 1.905 \times 3.175$ $B : SmCo, 2 \times 0.5$	M0900034, Tbl. 1
I_O^{req}	A	–	$T : 6 \times 10^{-2}$ $M : 3 \times 10^{-3}$ $B : 1.5 \times 10^{-4}$	T0900435, Tbl 1
A_O	N/A	–	T : 0.9630 M : 0.0158 B : 0.00281	"fmax," Tbls. 2 & 3, T1000164
$F_{max}^O = N_O\ I_O^{req}\ A_O$	N	$T : --$ $M : 2$ $B : 1 \times 10^{-6}$	$T : 1.156 \times 10^{-1}$ $M : 1.896 \times 10^{-4}$ $B : 1.686 \times 10^{-6}$	Calculated
$C_O^{F \to x}$	$(N/A)/m$	–	T : 87.6 M : 1.61 B : 0.288	"coupling," Tbls. 2 & 3, T1000164
$(dF/dx)/F = C_O^{F \to x}/A_O$	$1/m$	100	T : 90.97 M : 101.9 B : 102.5	Calculated
f_0	Hz	1.0	2.829	T080311
m_B	kg	3.5	2.892	T0900435, Sect. 9
$x_p(f)$	$m/\sqrt{Hz}$	1×10^{-11} @ 1 Hz 2×10^{-13} @ 10 Hz 5×10^{-15} @ 100 Hz	HAM ISI eLIGO Performance, aLIGO PRCL and SRCL Requirements	T0900285, Y Drxn. T1000216, Horz Drxn.

Table 2: HLTS Parameter Table.

Parameter	Units	HLTS T020059-v1	HLTS T020059-v2	v2 Reference
$x_B^{req}(f)$	$m\sqrt{Hz}$	4×10^{-16} @ 10 Hz, 1.5×10^{-17} @ 100 Hz	3×10^{-17} @ 10 Hz, Falling as $f^{-5/2}$	T010007
N_O	–	–	T : 2 M : 4 B : 4	T1000012, Tbl. 1
OSEM Type	–	$T : IOSEM$ $M : IOSEM$ $B : IOSEM$	$T : BOSEM$ $M : AOSEM$ $B : AOSEM$	M0900034, Tbl. 1
Magnet Type, Size	$mm \times mm$	$T : NdFeB, 1.905 \times 3.175$ $M : NdFeB, 1.905 \times 3.175$ $B : NdFeB, 1.905 \times 3.175$	$T : NdFeB, 10 \times 10$ $M : SmCo, 1.905 \times 3.175$ $B : SmCo, 2 \times 0.5$	M0900034, Tbl. 1
I_O^{req}	A	–	$T : 6.0 \times 10^{-2}$ $M : 3 \times 10^{-3}$ $B : 1.5 \times 10^{-4}$	T1000012, Tbl 1
A_O	N/A	–	T : 1.6940 M : 0.0158 B : 0.00281	"fmax," Tbls. 2 & 3, T1000164
$F_{max}^O = N_O\ I_O^{req}\ A_O$	N	$T : --$ M : 80 $B : --$	$T : 1.156 \times 10^{-1}$ $M : 1.896 \times 10^{-4}$ $B : 1.686 \times 10^{-6}$	Calculated
$C_O^{F \to x}$	$(N/A)/m$	–	T : 87.6 M : 1.61 B : 0.288	"coupling," Tbls. 2 & 3, T1000164
$(dF/dx)/F = C_O^{F \to x}/A_O$	$1/m$	100	T : 90.97 M : 101.9 B : 102.5	Calculated
f_0	Hz	1.0	2.899	T080310
m_B	kg	10	12.14	T1000012, Sect. 10
$x_p(f)$	$m/\sqrt{Hz}$	1×10^{-11} @ 1 Hz 2×10^{-13} @ 10 Hz 5×10^{-15} @ 100 Hz	HAM ISI eLIGO Performance, aLIGO PRCL and SRCL Requirements	T0900285, Y Drxn. T1000216, Horz Drxn.

4 Results

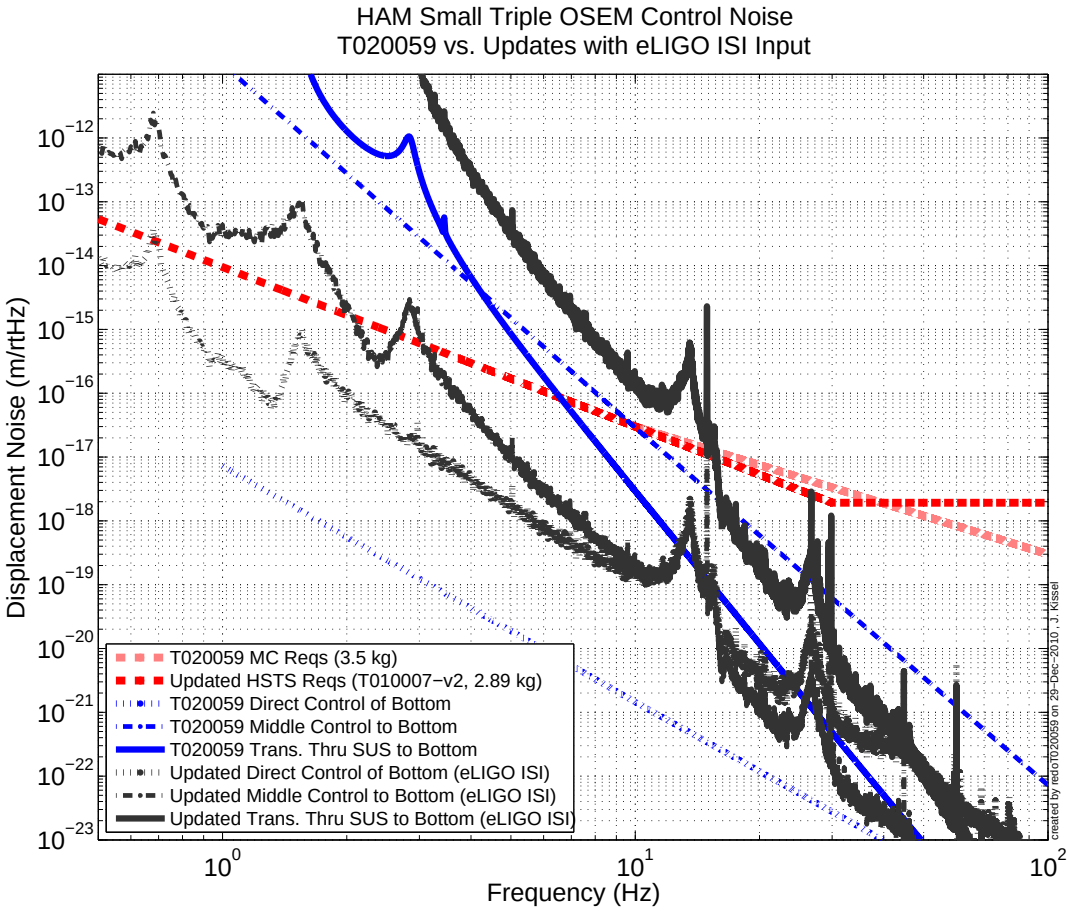

Figure 4: Predicted equivalent displacement noise of controlling the middle and bottom masses of the HSTS with OSEMs connected directly to the cage with the maximum possible force. Thick, red, dashed lines indicate the displacement noise requirements (defined in T020059-v1, and T010007/T080192). Solid lines indicate transmission of platform displacement noise through the triple suspension, $x_B^{p\rightarrow B}(f)$. Dash-dotted lines indicate the noise generated by OSEM control of the middle mass, $x_B^{O\rightarrow M\rightarrow B}(f)$, and dotted lines indicate noise generated by OSEM control directly on the bottom mass, $x_B^{O\rightarrow B}(f)$. Blue and gray colors delineate input platform motion, formed using that from T020059 and the performance of the eLIGO HAM ISI, respectively.

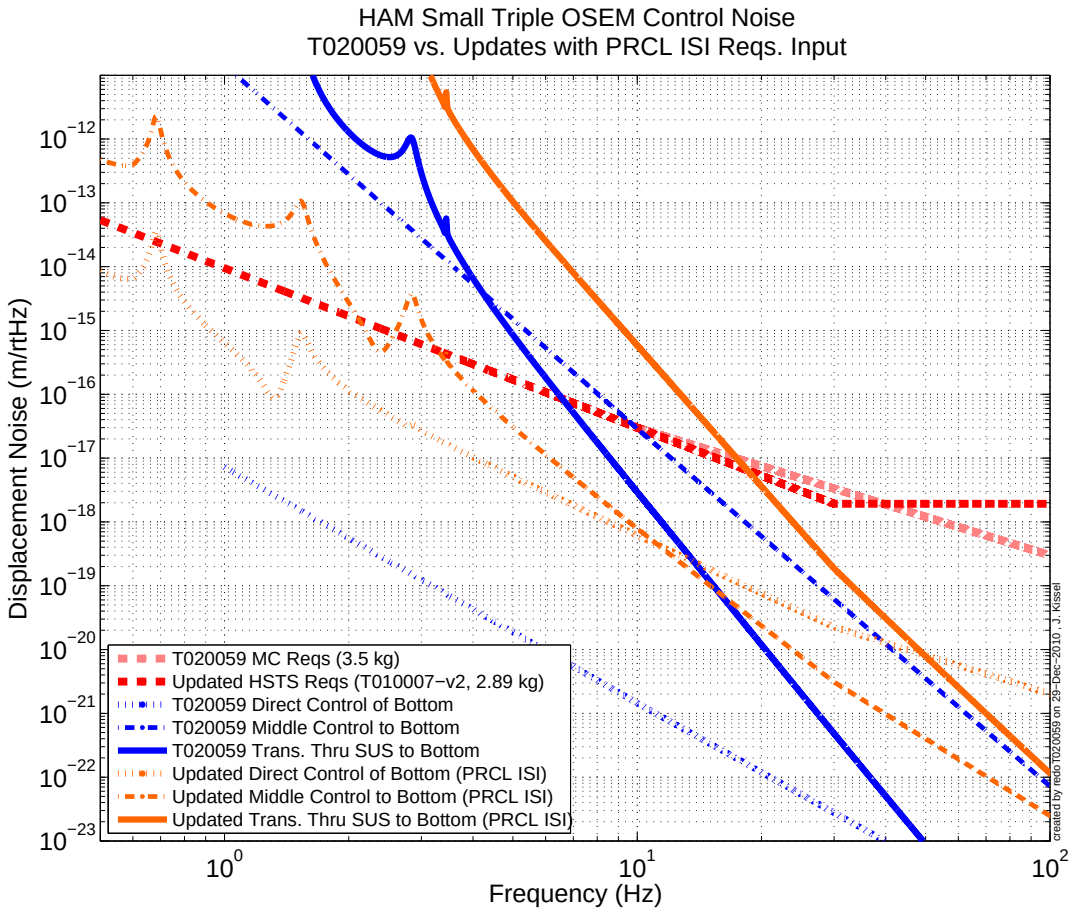

Figure 5: Predicted equivalent displacement noise of controlling the middle and bottom masses of the HSTS with OSEMs connected directly to the cage with the maximum possible force. Thick, red, dashed lines indicate the displacement noise requirements (defined in T020059-v1, and T010007/T080192). Solid lines indicate transmission of platform displacement noise through the triple suspension, $x_B^{p\rightarrow B}(f)$. Dash-dotted lines indicate the noise generated by OSEM control of the middle mass, $x_B^{O\rightarrow M\rightarrow B}(f)$, and dotted lines indicate noise generated by OSEM control directly on the bottom mass, $x_B^{O\rightarrow B}(f)$. Blue and orange colors delineate input platform motion, formed using that from T020059 and the performance of the PRCL HAM ISI, respectively.

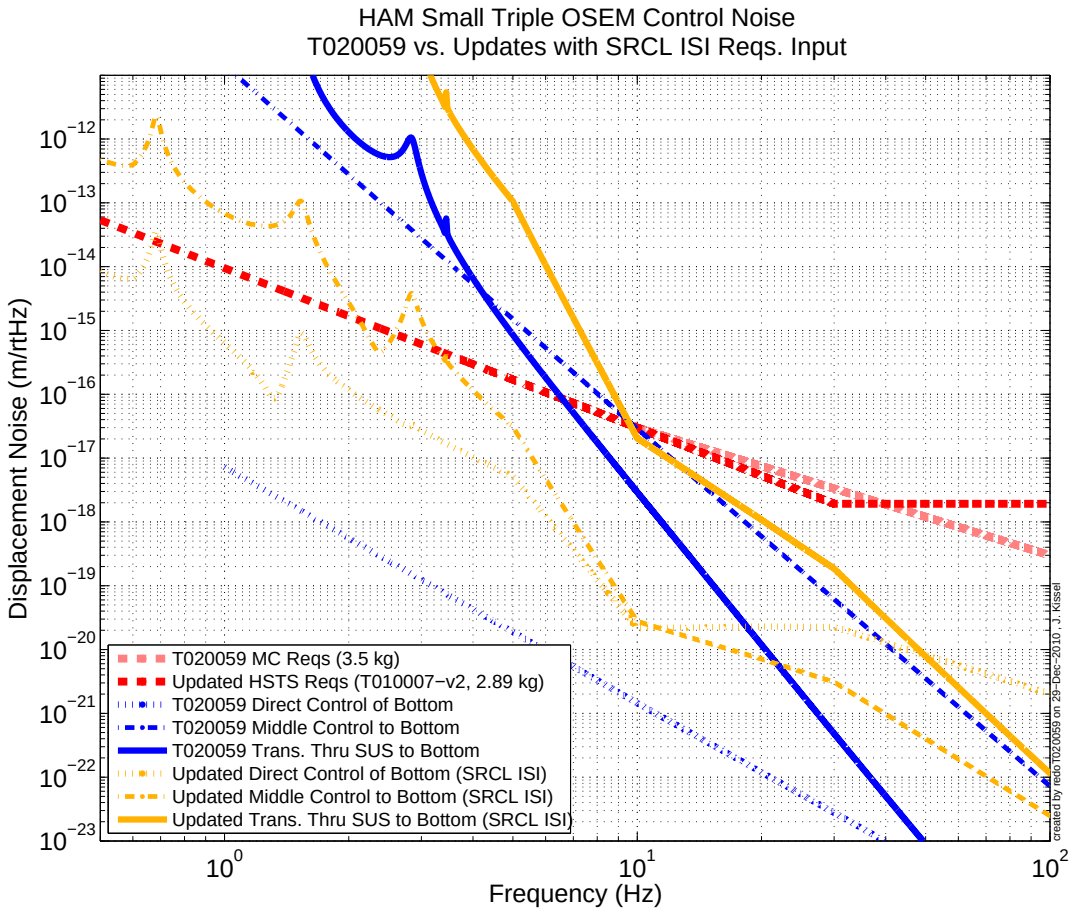

Figure 6: Predicted equivalent displacement noise of controlling the middle and bottom masses of the HSTS with OSEMs connected directly to the cage with the maximum possible force. Thick, red, dashed lines indicate the displacement noise requirements (defined in T020059-v1, and T010007/T080192). Solid lines indicate transmission of platform displacement noise through the triple suspension, $x_B^{p\rightarrow B}(f)$. Dash-dotted lines indicate the noise generated by OSEM control of the middle mass, $x_B^{O\rightarrow M\rightarrow B}(f)$, and dotted lines indicate noise generated by OSEM control directly on the bottom mass, $x_B^{O\rightarrow B}(f)$. Blue and gold colors delineate input platform motion, formed using that from T020059 and the performance of the SRCL HAM ISI, respectively.

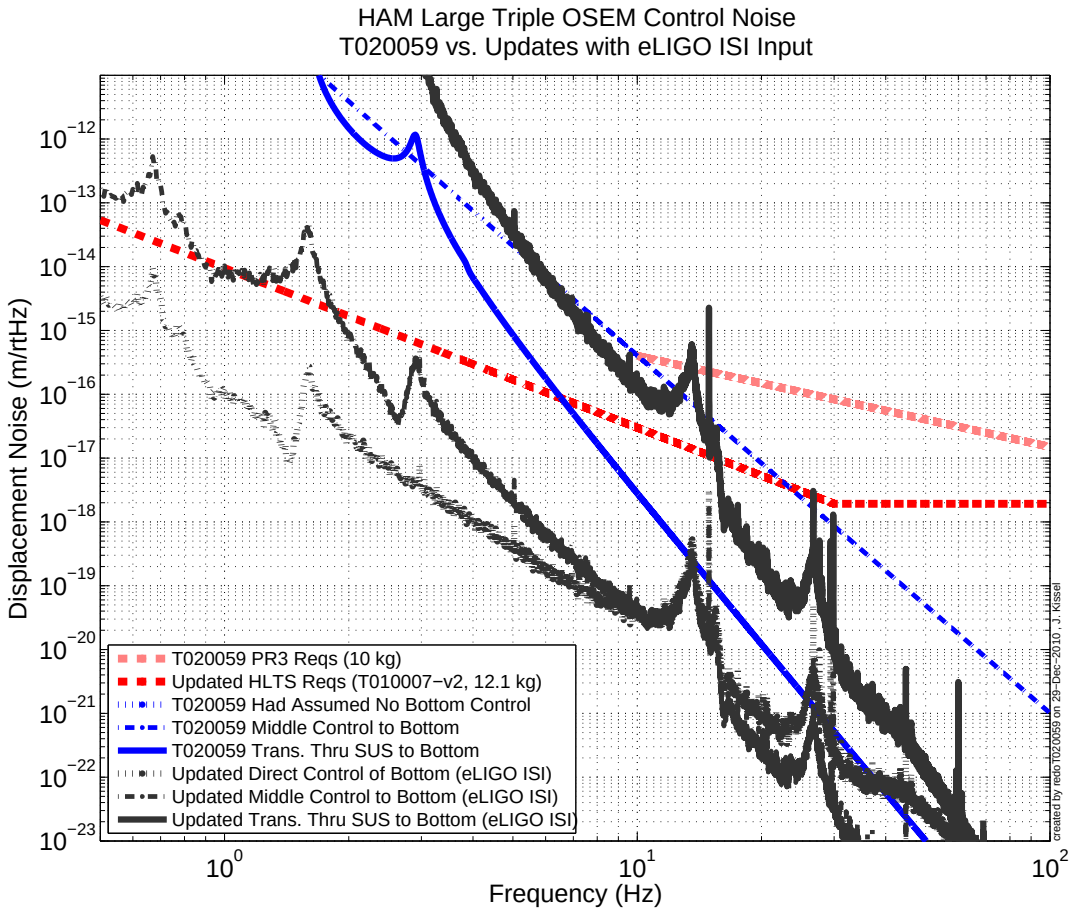

Figure 7: Predicted equivalent displacement noise of controlling the middle and bottom masses of the HLTS with OSEMs connected directly to the cage with the maximum possible force. Thick, red, dashed lines indicate the displacement noise requirements (defined in T020059-v1, and T010007/T080192). Solid lines indicate transmission of platform displacement noise through the triple suspension, $x_B^{p\rightarrow B}(f)$. Dash-dotted lines indicate the noise generated by OSEM control of the middle mass, $x_B^{O\rightarrow M\rightarrow B}(f)$, and dotted lines indicate noise generated by OSEM control directly on the bottom mass, $x_B^{O\rightarrow B}(f)$. Blue and gray colors delineate input platform motion, formed using that from T020059 and the performance of the eLIGO HAM ISI, respectively.

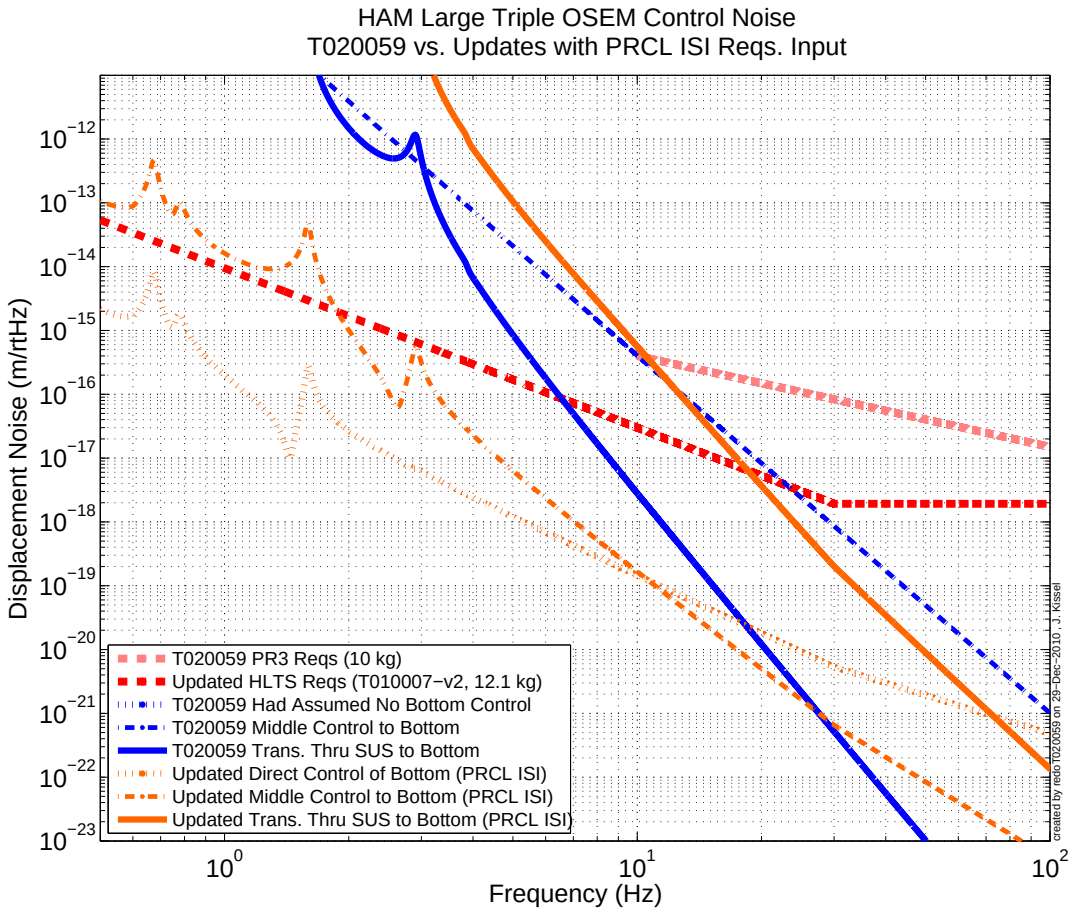

Figure 8: Predicted equivalent displacement noise of controlling the middle and bottom masses of the HLTS with OSEMs connected directly to the cage with the maximum possible force. Thick, red, dashed lines indicate the displacement noise requirements (defined in T020059-v1, and T010007/T080192). Solid lines indicate transmission of platform displacement noise through the triple suspension, $x_B^{p\rightarrow B}(f)$. Dash-dotted lines indicate the noise generated by OSEM control of the middle mass, $x_B^{O\rightarrow M\rightarrow B}(f)$, and dotted lines indicate noise generated by OSEM control directly on the bottom mass, $x_B^{O\rightarrow B}(f)$. Blue and orange colors delineate input platform motion, formed using that from T020059 and the performance of the PRCL HAM ISI, respectively.

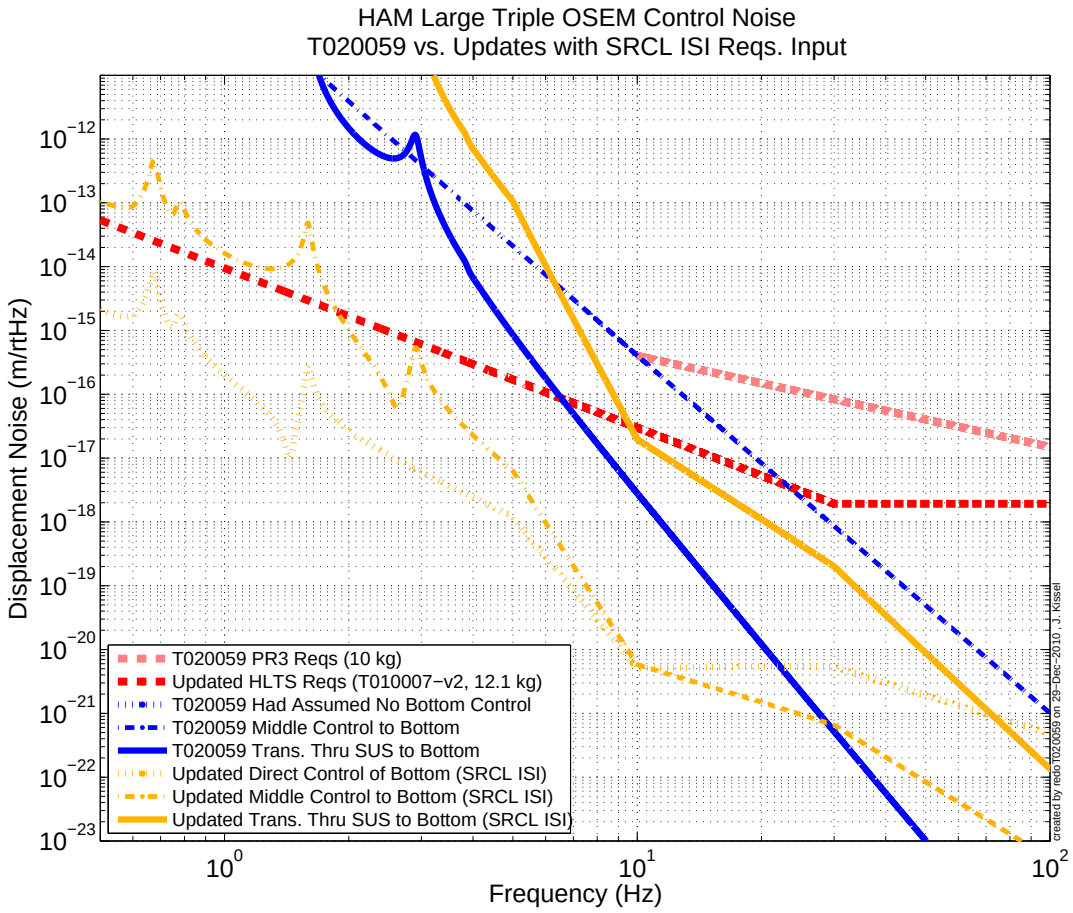

Figure 9: Predicted equivalent displacement noise of controlling the middle and bottom masses of the HLTS with OSEMs connected directly to the cage with the maximum possible force. Thick, red, dashed lines indicate the displacement noise requirements (defined in T020059-v1, and T010007/T080192). Solid lines indicate transmission of platform displacement noise through the triple suspension, $x_B^{p\rightarrow B}(f)$. Dash-dotted lines indicate the noise generated by OSEM control of the middle mass, $x_B^{O\rightarrow M\rightarrow B}(f)$, and dotted lines indicate noise generated by OSEM control directly on the bottom mass, $x_B^{O\rightarrow B}(f)$. Blue and gold colors delineate input platform motion, formed using that from T020059 and the performance of the PRCL HAM ISI, respectively.

5 Conclusions

Figures 4 through 9 demonstrate worst-case scenario control schema of controlling each stage of the HAM triples with OSEMs mounted directly to the cage. Assuming the force needed to control the optics is the maximum possible force that may be provided by the OSEMs, they will produce force noise below the equivalent length noise requirements for Advanced LIGO. It was thought that this worst-case force noise was $\sim$ 4 orders of magnitude away from the aLIGO requirements at 10 Hz. We have demonstrated that the noise resulting from the maximum control of the bottom mass is only $\sim$2 orders of magnitude away at 10 Hz (at worst, see Figure 5), but still comfortably below requirements. Further, the control noise for every input noise is well below the predicted model of transmission of platform motion through the triple suspensions; the "cross-over frequency" where this noise dominates is 50 Hz (70Hz) for every modeled input displacement to the HSTS (HLTS). We conclude that the discrepancy between Willems (2002) and this work is primarily due to the use of a two-stage isolation platform for input motion.

Examining the eLIGO HAM ISI platform motion below the HSTS shows, in some regions around HAM support structure resonances, the control noise on the bottom mass is as little as a factor of 5 away from the length requirements, which may be of concern. However, we must remember these calculations have described a worst-case scenario, with each OSEMs driving at their maximum. In reality, very little control will be applied to the lower stages of the suspension as there are many layers prior to the final stages on which control may be offloaded. Further, since the (re-)discovery of the HAM support structure resonances and their affect on the eLIGO HAM ISI performance, the support structure's cross-beams have been redesigned to be more stiff [10]. The aLIGO HAM chambers will also include additional isolation from HEPI which was not present for the prototypes. These enhancements should push the support structure resonances to higher frequencies, and reduce their Qs [12] such that their resonant features will contribute less to the force noise, likely to be reduced to just-above the "continuum" level noise at $\sim$ 2 orders of magnitude away from the requirements.

References

[1] P. Willems. "Are Reaction Chains Needed for AdLIGO HAM Optics?". LIGO Internal Document. LIGO-T020059-v1. (2002)

[2] M. Barton, N. A. Robertson, P. Fritshel, D. Shoemaker, P. Willems. "Cavity Optics Suspension Subsystem Design Requirements Document." LIGO Internal Document. LIGO-T010007. (2009)

[3] M. Evans, P. Fritschel. "Displacement Noise in Advanced LIGO Triple Suspensions." LIGO Internal Document. LIGO- T080192. (2008)

[4] N. A. Robertson, M. Barton, M. Meyer, J. Romie, C. Torrie. "HAM Small Triple Suspension Final Design Document." LIGO Internal Document. LIGO-T0900435. (2010)

[5] N. A. Robertson, D. Bridges, M. Barton, J. Heefner, J. Romie, C. Torrie. "HAM Large Triple Suspension (HLTS) Final Design Document." LIGO Internal Document. LIGO-T1000012. (2010)

[6] N. A. Roberston, P. Fritschel, J. Greenhalgh. "Magnet Sizes and Types and OSEM Types in Adv. LIGO Suspensions." LIGO Internal Document. LIGO-M0900034. (2010)

[7] M. Barton. "Calculation and Measurement of the OSEM Actuator Sweet Spot Position." LIGO Internal Document. LIGO-T1000164. (2010)

[8] J. Kissel, B. Lantz, N. A. Roberstion. "MATLAB Model of the HAM Large Triple Suspension (HLTS)." LIGO Internal Document. LIGO-T080310. (2010)

[9] J. Kissel, N. A. Roberstion. "MATLAB Model of the HAM Small Triple Suspension (HSTS)." LIGO Internal Document. LIGO-T080311. (2010)

[10] A. Stein, S. Foley, K. Mason. "HAM Crossbeam Redesign for Advanced LIGO: Impact on HAM Chamber Placement." LIGO Internal Document. LIGO-E080328. (2008)

[11] P. Fritschel, D. Coyne, J. Giaime, B. Lantz, D. Shoemaker. "Seismic Isolation Subsystem Design Requirements Document." LIGO Internal Document. LIGO-E990303.

[12] B. Lantz. "Revised HAM-ISI Performance Target for Advanced LIGO Signal Recycling Cavity Chambers." LIGO Internal Document. LIGO-T1000216. (2010)

[13] B. Lantz. "Inuence of HEPI and New Crossbeams on the 11.4 Hz Beam-Direction Peak." Seismic Group Electronic Log Entry #1287 `http://ligo.phys.lsu.edu:8080/SEI/1287`. (2008)